On Stability, Chirality Measures, and Theoretical VCD Spectra of the Chiral C58X2 Fullerenes (X = N, B)

ARTICLE *in* THE JOURNAL OF PHYSICAL CHEMISTRY A · NOVEMBER 2011

Impact Factor: 2.69 · DOI: 10.1021/jp208687c · Source: PubMed

4 AUTHORS, INCLUDING:

Michał Henryk Jamróz
Institute of Nuclear Chemistry and Technolo…
70 PUBLICATIONS **875** CITATIONS

SEE PROFILE

Joanna E Rode
Instytut Chemii Przemysłowej
38 PUBLICATIONS **516** CITATIONS

SEE PROFILE

THE JOURNAL OF PHYSICAL CHEMISTRY A

ARTICLE

pubs.acs.org/JPCA

On Stability, Chirality Measures, and Theoretical VCD Spectra of the Chiral $C_{58}X_2$ Fullerenes (X = N, B)

Sławomir Ostrowski,[†] Michał H. Jamróz,[†] Joanna E. Rode,[†] and Jan Cz. Dobrowolski*[,†,‡]

[†]Industrial Chemistry Research Institute, 8 Rydygiera Street, 01-793 Warsaw, Poland

[‡]National Medicines Institute, 30/34 Chełmska Street, 00-725 Warsaw, Poland

Supporting Information

ABSTRACT: The stability of all 23 $C_{58}N_2$ and $C_{58}B_2$ heterofullerenes in the singlet and triplet states was determined at the B3LYP/6-31G** level. In equilibrium mixture the achiral (1,4) $C_{58}N_2$ isomer would be populated in ca. 95.8%, the chiral (1,16) one in ca. 3.3%, and the achiral (1,4) $C_{58}B_2$ in 100%, whereas all triplet state isomers are less stable. Fourteen out of 23 $C_{58}X_2$ are chiral. Four different chirality measures were calculated by our own CHIMEA program: pure geometrical, labeled, mass, and charge. Intercorrelations between the measures for all chiral compounds indicate that the pure geometrical chirality measure is unstable and should not be used in QSAR predictions of the other molecular properties, while the labeled and mass-weighted ones are promising QSAR descriptors. For each chiral $C_{58}N_2$ molecule, some very strong VCD bands, of intensity comparable with that in the IR spectra, can serve in identification and characterization of the isomers.

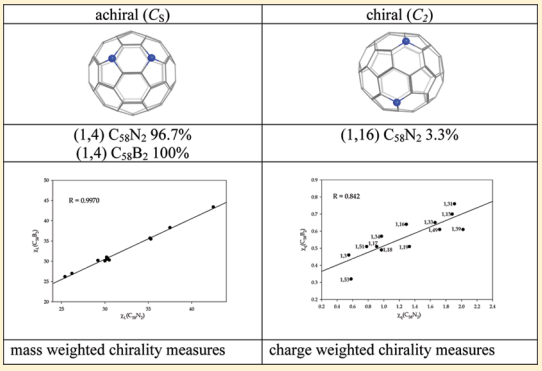

1. INTRODUCTION

Heterofullerenes are fullerenes with at least one atom replaced by a heteroatom.[1−4] They were first observed ($C_{60-n}B_n$; (n = 1−6)) by the Smalley group in the mass spectra of laser-vaporized graphite/boron nitride composites.[5,6] The Smalley group was also the first to observe the endohedral heterofullerenes (K@$C_{59}B$).[7] In 1995, the bulk preparation of $C_{59}N$ from its dimer $(C_{59}N)_2$ was developed by Hummelen et al.,[8] while a year later, Nuber and Hirsch elaborated a preparative method.[9] The $C_{59}N$ and $C_{58}N_2$ azafullerenes were synthesized by arc discharge under N_2 atmosphere by Yu et al.[10] A synthetic route toward $C_{58}N_2$ starting from C_{60} was proposed by the Hirsch group.[11,12] Now, up to 20% of $C_{58}N_2$ can be obtained by cycloaddition of a spacer-linked azide to the $C_{59}N$ core.[12] It has been shown that boron is more easily incorporated into carbon clusters and fullerenes than silicon[13] and that the predicted $C_{58}BN$ molecules[14,15] have been formed after laser ablation of C_2BN−graphite.[16] In 1997, the $C_{2n-1}Si$ fullerenes were observed by Fye and Jarrold,[17] and the $C_{2n-2}Si_2$ ones by Pellarin et al.[18] In 1999, Ohtsuki et al. detected formation of $C_{59}As$ and $C_{59}Ge$ by using radiochemical and radiochromatographic techniques.[19] Also, chemical functionalization of heterofullerenes is a mature field of synthetic fullerene chemistry.[1−4]

In 1995, Sjöström et al. demonstrated fullerene-like structures with incorporated nitrogen exhibiting exceptional hardness and very high film elasticities.[20] It is very likely that these properties are due to formation of the $C_{48}N_{12}$ dodecaazafullerene obtained by Hultman et al. in reactive magnetron sputtering of thin films of carbon nitride nano-onions.[21] For the $C_{60-n-m}N_nB_m$ heterofullerenes, Xie et al. showed the optical gaps and first triplet energies to be tunable from NIR to UV by tailoring the dopant numbers n and m and suggested the heterofullerenes to have potency as single-molecule fluorescent probes and as building blocks for the bottom-up assembly of tunable luminescent devices.[22] Interestingly, the electrical transport properties of C_{60} and $C_{59}N$ encapsulated SWNTs are different: in comparison to pristine SWNTs, C_{60}@SWNTs exhibit enhanced p-type characteristics, whereas $C_{59}N$@SWNTs show n-type behavior.[23]

The $C_{58}N_2$ and $C_{58}B_2$ heterofullerenes have been studied since the early 1990s. Influence of donor−acceptor properties of the B and N atoms on electronic structures of $C_{58}N_2$ and $C_{58}B_2$ solids was calculated using the tight-binding approximation.[24] Splitting of the HOMO and LUMO levels in $C_{58}N_2$ and $C_{58}B_2$ different than in bare C_{60} molecule was presented by DFT calculations within the local density approximation.[25] The electron-binding energies of $C_{58}N_2$ and $C_{58}B_2$ were calculated by a self-consistent-Geld method, to be much smaller and about the same (ca. 5.91 and 6.02 eV/atom, respectively) than that of C_{60} (6.05 eV/atom), whereas the HOMO−LUMO energy gaps, 1.50 eV for C_{60}, were estimated to be much smaller: ca. 0.25 and 0.52 eV, respectively.[26] The $C_{58}B_2$ and $C_{58}N_2$ electronic properties in solids were studied by Su−Schrieffer−Heeger model extended from that for C_{60}, obtaining good agreement with the SCF results except for a $C_{58}B_2$ isomer with B atoms on opposite

Received: September 8, 2011
Revised: November 9, 2011
Published: November 11, 2011

sides of the molecule.[27] Orbital correlation diagrams for 5−6′ and 6−6′ isomers of $C_{58}B_2$ and $C_{58}N_2$ were studied by the extended Hückel method.[28] It was also suggested that the 6−6′ $C_{58}N_2$ isomer is more stable than the 5−6′ one, while for $C_{58}B_2$ the opposite.[28] In the early 2000s, the XPS and NEXAFS spectra were predicted for four $C_{58}N_2$ isomers by DFT calculations showing strong isomer dependence of the spectra.[29] The second hyperpolarizability of the $C_{58}B_2$, $C_{58}N_2$, and $C_{58}BN$ molecules studied at the TD-DFT level suggested that the important changes (about 50%) can be expected only when both B and N atoms are incorporated into the molecule.[30]

So far, limited experimental data of interest to materials science exist for $C_{58}X_2$. In most studies on $C_{58}X_2$ compounds at most only a few isomers were investigated, whereas there are possibly as many as 23 different $C_{58}X_2$ isomers preserving the isolated pentagon rule (IPR).[1] In very complete studies, much more structures would be considered for the presence of heteroatoms, making some of the IPR violating isomers quite likely to be detected.[31] Two papers published in 1998 by Chen et al.[32,33] presented a systematic semiempirical (AM1, PM3, MNDO, and INDO) investigation of all the IPR conserving $C_{58}B_2$ and $C_{58}N_2$ isomers. For all of these isomers they calculated the equilibrium geometrical structures, heats of formation, HOMO−LUMO gaps, heats of atomization, ionization potentials, and affinity potentials. It appeared that the (1,4) isomer of $C_{58}B_2$ and $C_{58}N_2$ is the most stable and that roughly the stability decreases with the increasing distance between the heteroatoms. Also, nitrogen derivatives were suggested to be more stable than the boron ones; however, stabilities of $C_{58}BN$ isomers are considerably higher than that of $C_{58}X_2$. In comparison with the parental C_{60} molecule, the $C_{58}X_2$ isomers exhibit smaller ionization and larger affinity potentials. The electronic spectra of all the structures studied were calculated using the INDO/CIS method approach. Quite recently, Fan et al. have systematically studied the $C_{60-n}Si_n$ structures computationally and found, for example, that out of the 23 $C_{58}Si_2$ isomers, the (1,4) one is the stablest and (1,3) and (1,7) forms are energetically low-lying species.[34] They also found that for $2 < n < 30$ the Si atoms in the heterofullerene cages tend to aggregate and chemical ordering is not a primary factor for stability of the $C_{60-n}Si_n$ structures.[34]

Incorporation of a heteroatom into fullerenes gives the possibility to adjust their properties by changing curvature, charge distribution in molecule, electronic state, and thus the electric and magnetic properties (for odd n, $C_{60-n}X_n$, X = N, B are likely to be the open shell systems),[35] optical properties, chemical reactivity, ability to form fullerene onionlike superstructures, and solid phase properties such as hardness and elasticity, etc. Presence of heteroatoms may also stabilize structures for which the isolated pentagon rule is violated.[31] Fullerene chirality is also a property which can additionally enrich the range of their possible useful features.

Chirality is a property of molecules that has attracted increasing attention, mostly because of biological and pharmaceutical significance of enantiopure compounds.[36,37] Pharmaceutical activity of chiral compounds is also the main driving force in developing asymmetric synthesis[38] and asymmetric catalysis.[39,40] A fullerene molecule can be chiral per se if it does not have an orientation-reversing self-isometry (has neither a mirror plane nor a symmetry center nor an n-fold inversion axis). The first chiral fullerenes, D_2-symmetry C_{76}[41] and D_3-symmetry C_{78},[42] were isolated and characterized in the early 1990s. Fullerenes can also become chiral by functionalization.[43] Incorporation of heteroatoms into an achiral parent fullerene can also make it chiral. Indeed, out of 23 different $C_{58}X_2$ molecules, 14 are chiral, so including each of the two separate enantiomers, there are 37 different $C_{58}X_2$ diheterofullerenes.[44]

Careful reading of the recent review article entitled "*Quantitative Correlation of Physical and Chemical Properties with Chemical Structure: Utility for Prediction*" by the Katritzky group[45] would suggest that chirality is an unimportant parameter in QSAR analyses. Indeed, in over 70 pages of this review, this very property had not been mentioned even once. On the other hand, the number of chiral drugs increases, and the pharmaceutical industry intensively introduces more and more enantiopure analogues of known racemic drugs. Also, a huge effort is made to improve methods of asymmetric synthesis. So far, the majority of QSAR analyses of chiral substances are performed based on so-called topological indices corrected for chirality.[46−48] However, topological indices contain only indirect information on spacial properties of molecules, and we expect that indices more closely related to 3D molecular structure may perform better. A practical method for calculation of chirality measures is enabled only for so-called *Continuous Chirality Measure* by only one computer program of the Avnir group being accessible through the following web page: http://www.csm.huji.ac.il/.[49] However, only molecules up to 30 atoms can be examined by this program. Recently, we have developed the CHIMEA program which calculates different chirality measures: purely geometrical, labeled, mass, and charge weighted. In our program, a molecule is considered as a set of points in the Cartesian product of the R^3 and P^k spaces, where P^k is the *property space*. The distance between two points in the $R^3 \times P^k$ space is assumed to be defined by ordinary Cartesian distance in which the properties p^1, ..., p^k are the fourth, ..., kth coordinates from the P^k subspace. The chirality measure of a so-defined molecule is a minimized distance between the molecule and its mirror image. In this paper, we show properties of the newly proposed chirality measures applied to rigid chiral systems such as chiral $C_{58}X_2$ heterofullerenes.

The aim of this paper was threefold: (i) to estimate which of the chiral $C_{58}X_2$ heterofullerenes (X = N, B) is supposed to be the most populated in the equilibrium mixture; (ii) to characterize the $C_{58}X_2$ fullerene chirality by chirality measures developed by us recently; and (iii) to indicate the method enabling detection and differentiation of the studied chiral heterofullerenes. Additionally, by comparison of different chirality measures for various $C_{58}X_2$ structures we were able to discuss properties of these measures themselves. We think that the more promising properties of heterofullerenes are found by computational studies, the more the synthetic heterofullerene chemistry is provoked to elaborate larger amounts of these compounds. It is known that carbon nanotubes change electronic properties from metals to semiconductors depending on their chiral vectors.[50] Recent findings showing that C_{60}@SWNTs exhibit enhanced p-type characteristics compared with the case of pristine SWNTs, whereas $C_{59}N$@SWNTs show the n-type behavior,[51] indicates that new exciting features of heterofullerenes are still being discovered and some unexpected characteristics of chiral heterofullerenes are waiting to be found.

2. CALCULATIONS

2.1. Quantum Chemical Calculations. The quantum chemical calculations were performed by using the B3LYP and UB3LYP methods[52,53] combined with the 6-31G** basis set[54]

as implemented in the Gaussian 09 suite of programs.[55] None of the optimized structures exhibited imaginary frequency; thus, all of them are true energy minima at the level of theory applied. The isomer population was calculated based on Gibbs free energies, the Boltzmann distribution function, gas constant equal to 0.001 987 kcal mol^{-1} K^{-1}, and temperature set at 298 K. As with an excellent accuracy the enantiomers are equally stable, we calculated only one out of two enantiomer structures. The IR and vibrational circular dichroism (VCD) spectra were calculated based on Gaussian 09 codes.[56] The spectra analysis was followed by the PED performed with the VEDA (vibrational energy distribution analysis) program.[57] We intended to make an assignment of the most intense modes based on PED analysis, yet the internal coordinates resulted from such an analysis appeared to be too complex to yield a proper and clear description of the modes.

2.2. Chirality Measures Calculations. Chirality measures were calculated by using the CHIMEA program[58] which is based on similarity measure between enantiomers measured as minimized (weighted) distance (1)

$$\chi(A) = \frac{1}{a} \cdot \min_{g \in \mathrm{Tr} \circ \mathrm{SO}(3)} \left(\sum_f w_{i\pi_i} d(a_i, g(\sigma(a_{\pi_i}))) \right) \quad (1)$$

where Tr is an arbitrary translation, SO(3) is an even isometry-preserving position of a chosen point, g is a composition of Tr and SO(3), min is minimization running over all possible g, d is a distance between points a_i and $\sigma(a_{\pi i})$, σ is reflection against an arbitrary plane, π_i is a permutation of the index i running over numbers from 1 to n, w_i is a weight of ith distance, a normalizes the measure, and Σ_f denotes summing over all possible permutation of indices.

The distance d between the points a_i and $\sigma(a_{\pi i})$ can be defined as a Cartesian distance between two points in the $R^3 \times P^k$ space, assuming the x, y, and z to be coordinates of the object in R^3 and the properties p^1, ..., p^k to be the fourth, ..., kth coordinates from the P^k subspace. Then the distance d_i may be defined naturally as

$$d_i = \sqrt{(x_i - \overline{x_i})^2 + (y_i - \overline{y_i})^2 + (z_i - \overline{z_i})^2 + (p_i^1 - \overline{p_{i_i}^1})^2 + \ldots + (p_i^k - \overline{p_{i_i}^k})^2} \quad (2)$$

where the $\sigma(a_{\pi i})$ symbol is replaced by a less formal $\overline{p_i}$.

To understand the meaning of the expression 2 it is necessary to explain the action of symmetry plane on property p_i, i.e., meaning of symbol $\overline{p_i}$, rules for algebraic operations on p_i, in particular the results of subtraction $p_i - \overline{p_i}$ and addition $\Sigma_{i=1}^{n} p_i$, and multiplication by numbers necessary for preserving uniformity of physical units of d_i. For properties such as charge and mass these operations are obvious. However, for properties such as for example "color" of the points or "charm", etc., the additional rules, defining algebraic operations acting on this very propery, such as "$\overline{blue}$" = "red" and "blue"−"red" = 3, etc., have to be postulated. Having all of these definitions, congruency of the physical unit can be simply introduced by linear coefficients α_i converting p_i into p_i' and changing unit U into U' (for example, g into Å). In this way, the chirality measure may still be defined by eq 1.

For chemistry a property of a point is important indeed. First of all, the property can be understood as the "label" of the point (name of chemical element) differentiating various types of points. Here, we consider the following properties of points (atoms): atom type (label) (t_i), mass (m_i), charge (q_i), and connectivity index (c_i). The sets of atom types and masses are finite, whereas charges can change smoothly. A connectivity index depends on the valency of a point (understood as a vertex of a graph embedded in R^3) and its connection mode with the adjacent points. Here, we assume $t_i = \overline{t_i}$, $m_i = \overline{m_i}$, $q_i = \overline{q_i}$, and $c_i = \overline{c_i}$ and assume the following distances ρ between the property and its image:

$$\rho(p_i - \overline{p_i}) = \begin{cases} 0 & \text{if and only if } p_i = \overline{p_i} \\ \infty & \text{otherwise} \end{cases}, \text{where } p_i = t_i, m_i, q_i, c_i \quad (3)$$

Note that using such discrete measures additional unit-converting coefficients need not be defined, because for both values they are meaningless. Definition 3 guarantees that minimization condition can be satisfied if and only if the proper atoms are paired by mirroring. However, considering a measure taking more than only two values can be useful to express a gradation within a property. It seems that, in particular, the third value of 1 (after the unit conversion) might represent a useful compromise between all and nothing.

In the chirality measure minimization routine distances between different points in a molecule and its mirror image are measured. The compared points are changed and number of comparisons increases rapidly with the number of points that have to be compared. Definitions of different measures tell us which points can be compared and which cannot. So, for purely geometrical measure every point from a chiral set can be compared with every point in the mirror image, while in the labeled measure only points with the same label in the set and its image can be compared. The same holds for mass and charge chirality measures.

For "real" molecules determination of chirality is, however, a bit more complicated than that defined by expression 1. It often happens that in a crystal a molecule occupies two or more nonequivalent positions and occurs in different forms. In such a case, the chirality of a molecule A in a crystal phase K, $\chi(A(K))$, can be understood as the value averaged over all k-nonequivalent structures of A in the elementary cell

$$\chi(A(\mathrm{K})) = \frac{1}{k} \sum_{i=1}^{k} l_i \cdot \chi(A_i) \quad (4)$$

where l_i is number of molecule A_i in the elementary cell. Obviously, for a flexible molecule in the gas, liquid, and dissolved phases the expression should be modified and l_i should denote the Boltzmann population factors.

2.3. Description of the CHIMEA Program Calculating Chirality Measures of a Molecule. In the CHIMEA program geometric, mass, and charge chirality measures have been defined based on definitions 1−3. In these measures the normalization factors are either number of atoms, sum of atomic masses, or sum of absolute values of charges. (We consider also mass chirality in a square root variant in which square roots of masses are used in both weights and normalization factors.) In the program we use a modification of a distance in the following form:

$$d_i^w = \sqrt{(w_i x_i - \overline{w_i x_i})^2 + (w_i y_i - \overline{w_i y_i})^2 + (w_i z_i - \overline{w_i z_i})^2 + (p_i - \overline{p_i})^2} \quad (2a)$$

which reduces to $w_i d_i$ when $w_i = \overline{w_i}$ but is slightly different if we allow comparison of different properties. In expression 2a w denotes mass, square root of mass, or charge of the ith atom and ith atom in the image, whereas p_i is connectivity up to second and fourth order.

dx.doi.org/10.1021/jp208687c | J. Phys. Chem. A 2012, 116, 631–643

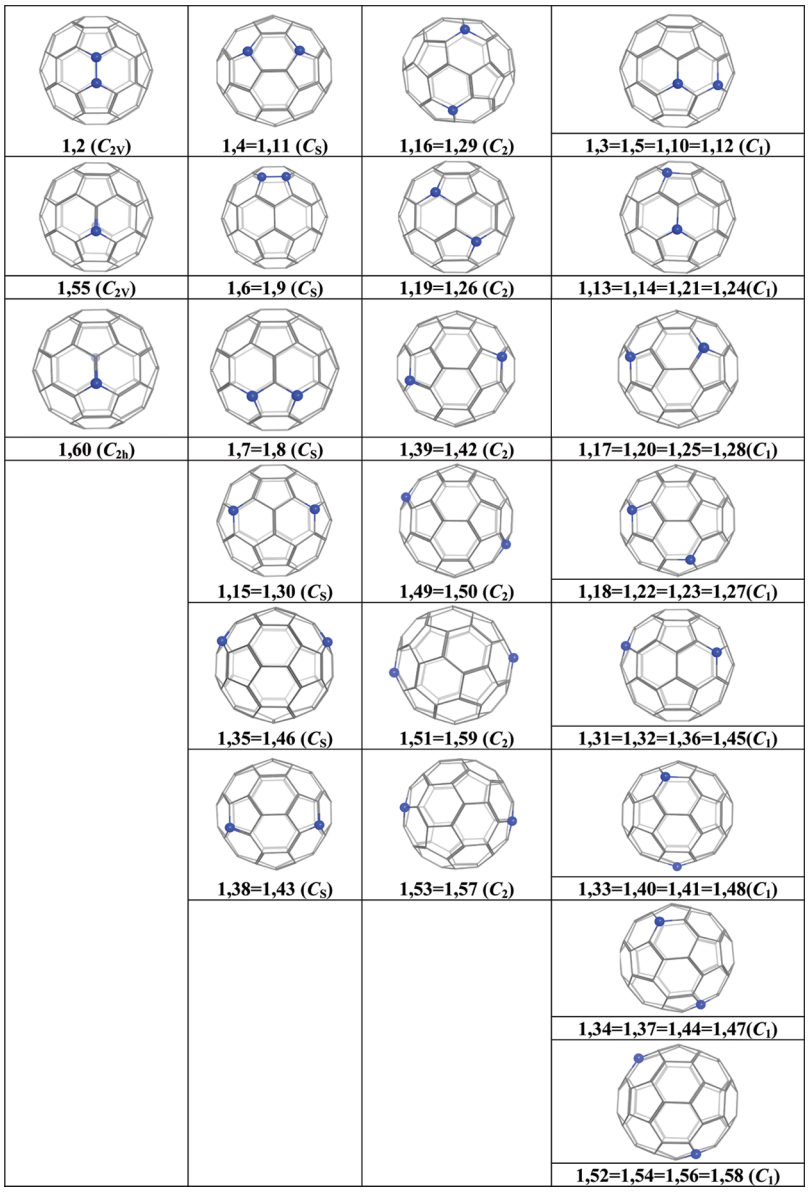

Figure 1. The 23 possible $C_{58}X_2$ heterofullerenes (atom numbering according to IUPAC rules). The group symmetry symbols (C_1 and C_2) indicate selected enantiomers of 14 chiral isomers.

In the first step, the center of a molecule, represented by *n*-points in the Cartesian coordinates, is translated to the origin of coordinates. Next the molecule is so rotated that the sum of the absolute values of *Z*-coordinates (SAZ) is minimal, and next the molecule is rotated about the *Z*-axis to minimize the sum of the absolute values of *Y*-coordinates (SAY). In this procedure SAZ ≤ SAY ≤ SAX. In this moment the mirror image against the *XY*-plane is generated, and the starting value of the measure is calculated. This measure is iteratively minimized in alternation of translations and rotations about the *Z*- axis. At the end of this step a slight wagging of the *Z*-axis is enforced. The routine is repeated several times. The key feature of the measure is the proper pairing of the points of the molecule and the points in its mirror image. Note that the pairing have not been necessarily between the point and its factual mirror image, and only the molecular graph isomorphism preservation has to be satisfied.

In search of the measure, several local and global minima can be found. To increase possibility of finding the global minimum, several starting arrangements of the image against the molecule are considered. To select the starting arrangements of "ball-like" structures, i.e., for structures for which SAZ/SAX ≥ 0.3, the Monte Carlo routine additionally generates several hundreds of hazardous rotations of the *Z*-axis.

Similar steps are done in estimating the mass and charge measures. As a result we obtain four measures, purely geometrical, labeled (by atomic symbols), mass, and charge chirality measure, and the geometrical arrangement of the molecule and its image for which each of the measures was obtained. Usually, we assume Cartesian distance (2a) in which the type of atom and type of atom connectivity are "switched on", while atomic mass and charge are "switched off".

In calculations, the properties can be taken into account or not. In the pure geometrical chirality measure the weights are assumed to be 1, whereas in the mass and charge chirality measures the weights are mass or charge dependent. Because the properties are

Table 1. B3LYP/6-31G Calculated Gibbs Free Energies (G_{298}, Hartree) for the $C_{58}N_2$ and $C_{58}B_2$ Isomers in the Singlet and Triplet States and Relative Energies Taken against the Most Stable (1,4) Isomer (ΔG_{298}, kcal/mol) as Well as Their Equilibrium Content at 298 K (mol %)**

$C_{58}N_2$								$C_{58}B_2$							
		singlet state			triplet state					singlet state			triplet state		
isomer	sym.	G_{298}	ΔG_{298}	popul.	G_{298}	ΔG_{298}	popul.	isomer	sym.	G_{298}	ΔG_{298}	popul.	G_{298}	ΔG_{298}	popul.
(1,2)	C_{2v}	−2319.072713	15.2	0.00	−2319.031802	32.5	0.00	(1,2)	C_{2v}	−2259.306629	17.7	0.00	−2259.273326	22.4	0.00
(1,3)	C_1	−2319.079024	11.2	0.00	−2319.069546	8.8	0.00	(1,3)	C_1	−2259.303893	19.4	0.00	−2259.308824	0.1	23.59
(1,4)	C_s	−2319.096899	0.0	95.82	−2319.061597	13.8	0.00	(1,4)	C_s	−2259.334768	0.0	100.00	−2259.307267	1.1	2.26
(1,6)	C_s	−2319.046696	31.5	0.00	−2319.043130	25.4	0.00	(1,6)	C_s	−2259.287591	29.6	0.00	−2259.282860	16.4	0.00
(1,7)	C_s	−2319.075218	13.6	0.00	−2319.071678	7.5	0.00	(1,7)	C_s	−2259.311025	14.9	0.00	−2259.309025	0.0	14.59
(1,13)	C_1	−2319.087134	6.1	0.01	−2319.069546	8.8	0.00	(1,13)	C_1	−2259.305281	18.5	0.00	−2259.305007	2.5	0.41
(1,15)	C_s	−2319.082738	8.9	0.00	−2319.082848	0.5	15.60	(1,15)	C_s	−2259.319931	9.3	0.00	−2259.304427	2.9	0.11
(1,16)	C_2	−2319.093709	2.0	3.26	nc[a]	–	–	(1,16)	C_2	−2259.303531	19.6	0.00	−2259.306468	1.6	0.97
(1,17)	C_1	−2319.088381	5.3	0.02	−2319.073377	6.4	0.00	(1,17)	C_1	−2259.301176	21.1	0.00	−2259.307080	1.2	3.71
(1,18)	C_1	−2319.083386	8.5	0.00	nc	–	–	(1,18)	C_1	−2259.308252	16.6	0.00	−2259.306016	1.9	1.20
(1,19)	C_2	−2319.087073	6.2	0.00	−2319.070830	8.0	0.00	(1,19)	C_2	−2259.304458	19.0	0.00	−2259.300429	5.4	0.00
(1,31)	C_1	−2319.082376	9.1	0.00	−2319.077259	3.9	0.08	(1,31)	C_1	−2259.301363	21.0	0.00	−2259.308299	0.5	13.52
(1,33)	C_1	−2319.078786	11.4	0.00	−2319.076511	4.5	0.04	(1,33)	C_1	−2259.301576	20.8	0.00	−2259.308259	0.5	12.96
(1,34)	C_1	−2319.086226	6.7	0.00	−2319.081233	1.5	5.63	(1,34)	C_1	−2259.303430	19.7	0.00	−2259.308099	0.6	10.94
(1,35)	C_s	−2319.092473	2.8	0.88	−2319.080065	2.2	0.82	(1,35)	C_s	−2259.315191	12.3	0.00	−2259.305274	2.4	0.27
(1,38)	C_s	−2319.084108	8.0	0.00	−2319.070488	8.2	0.00	(1,38)	C_s	−2259.305759	18.2	0.00	−2259.306024	1.9	0.61
(1,39)	C_2	−2319.079823	10.7	0.00	nc	–	–	(1,39)	C_2	−2259.296939	23.8	0.00	−2259.305966	1.9	0.57
(1,49)	C_2	−2319.080079	10.6	0.00	−2319.078303	3.3	0.13	(1,49)	C_2	−2259.300513	21.5	0.00	−2259.307837	0.7	4.14
(1,51)	C_2	−2319.084837	7.6	0.00	−2319.076761	4.3	0.02	(1,51)	C_2	−2259.305621	18.3	0.00	−2259.307139	1.2	1.98
(1,52)	C_1	−2319.083775	8.2	0.00	−2319.083601	0.0	69.32	(1,52)	C_1	−2259.303450	19.7	0.00	−2259.307817	0.8	8.11
(1,53)	C_2	−2319.087071	6.2	0.00	−2319.082205	0.9	7.89	(1,53)	C_2	−2259.310304	15.4	0.00	−2259.293005	10.1	0.00
(1,55)	C_{2v}	−2319.087670	5.8	0.00	−2319.067928	9.8	0.00	(1,55)	C_{2v}	−2259.309696	15.7	0.00	−2259.303919	3.2	0.03
(1,60)	C_{2h}	−2319.085702	7.0	0.00	−2319.080160	2.2	0.45	(1,60)	C_{2h}	−2259.307283	17.3	0.00	−2259.300986	5.0	0.00

[a] nc stands for not converged structure.

considered to be independent from one another for each chirality measure one can consider $2^4 = 16$ different distances between the points. Formally, because for each three general types of measures minimization ends up in geometrical arrangement of the molecule and its translated and rotated image, each type can be calculated in geometry fixated from different minimization conditions which gives as much as 144 different values ($16 \times 3 \times 3$). In practice, we limit our consideration to pure, labeled, mass, and charge chirality measures.

3. RESULT AND DISCUSSION

3.1. Energetics and Conformer Population. In 1998 Chen et al. calculated all the IPR-conserving $C_{58}N_2$ and $C_{58}B_2$ isomers in the singlet state at the AM1, PM3, MNDO, and INDO semiempirical levels.[32,33] More than a decade later, their findings can be verified at a more trustable DFT level. The Gibbs free energies and relative Gibbs free energies of all studied isomers (Figure 1, the isomers were named after IUPAC recommendation[59]), in the singlet and triplet states, calculated at the B3LYP/6-31G** level are juxtaposed (Table 1).

According to the point group symmetry, the 23 $C_{58}X_2$ isomers are split out into the C_1, C_2, C_s, C_{2v}, and C_{2h} type of structures, populated by 8, 6, 6, 2, and 1 isomer, respectively (Figure 1, Table 1). The C_1 and C_2 symmetry structures are chiral, and thus, in fact, there are eight and six pairs of enantiomers, respectively. For a symmetry plane that is an element of the C_s, C_{2v}, and C_{2h} groups, the nine structures belonging to these very groups are achiral.

Surprisingly, the main Chen et al. result for the $C_{58}N_2$ isomers,[32,33] i.e., the energetic order of the two most populated conformers (in the singlet state) remains valid. Indeed, the (1,4) $C_{58}N_2$ isomer is the most stable, and the (1,16) one is the next stable (Table 1). The former is estimated to be populated in ca. 95.8%, belongs to the C_s symmetry group, and thus is achiral, whereas the latter is estimated to be populated in ca. 3.3%, belongs to the C_2 group, and is chiral. The third one, the achiral (1,35) isomer of C_s symmetry, is populated in ca. 0.9%. Out of the other isomers, in the singlet state, only (1,13) and (1,17) isomers belonging to the C_1 group of symmetry are populated in minute amounts (a matter of 0.01 and 0.02%, respectively).

For the $C_{58}N_2$ isomers with the N atoms separated by a few bonds, the presence of biradical forms as well as population of the triplet states seems not to be unlikely. Therefore, we optimized all but not converging three ((1,16), (1,18), and (1,39) isomers) in their triplet states (Table 1) and found that, at the B3LYP/6-31G** level, all of them are less stable than the two most stable singlet state forms. However, if the triplet state forms would be separated from the singlet ones, the chiral (1,52) isomer (C_1) could be populated in almost 70%, and the achiral (1,15) and chiral

Table 2. Different Types of Chiralities Calculated for the Chiral $C_{58}N_2$ and $C_{58}B_2$ Isomers in Singlet and Triplet States Based on the B3LYP/6-31G Calculated Data by Using the CHIMEA Program[a]**

	geometry-based chirality measures					geometry-based chirality measures			
$C_{58}N_2$ isomer	χ_0	χ_L	χ_m	χ_q	$C_{58}N_2$ isomer in triplet state	χ_0	χ_L	χ_m	χ_q
(1,3)	1.83	30.3	365.4	0.55	(1,3)	1.40	30.3	365.4	0.58
(1,13)	0.71	29.2	352.8	1.88	(1,13)	2.05	29.2	352.8	1.87
(1,16)	**1.34**	**37.5**	**451.8**	1.29	**(1,16)**	nc	nc	nc	nc
(1,17)	1.57	35.3	424.7	0.91	(1,17)	0.00	35.3	424.9	0.83
(1,18)	1.11	30.2	364.4	0.97	(1,18)	nc	nc	nc	nc
(1,19)	1.14	30.5	367.7	1.33	(1,19)	1.12	30.5	367.7	1.25
(1,31)	1.27	30.0	362.4	1.91	(1,31)	1.55	30.0	362.4	1.88
(1,33)	1.70	26.2	317.5	1.20	(1,33)	1.61	26.2	317.6	1.21
(1,34)	1.42	35.2	424.0	0.97	(1,34)	1.03	35.3	425.1	0.96
(1,39)	1.47	42.5	509.8	2.02	(1,39)	nc	nc	nc	nc
(1,49)	0.91	25.4	307.3	1.72	(1,49)	1.24	25.4	307.3	1.75
(1,51)	1.17	30.2	363.6	0.78	(1,51)	1.21	30.1	362.9	0.68
(1,52)	1.06	40.5	485.5	2.39	(1,52)	1.24	40.4	484.8	2.27
(1,53)	1.58	35.2	424.4	0.58	(1,53)	1.04	35.4	426.5	0.43

	geometry-based chirality measures					geometry-based chirality measures			
$C_{58}B_2$ isomer	χ_0	χ_L	χ_m	χ_q	$C_{58}N_2$ isomer in triplet state	χ_0	χ_L	χ_m	χ_q
(1,3)	1.78	30.8	368.5	0.46	(1,3)	1.68	30.6	366.5	0.33
(1,13)	3.32	30.2	361.3	0.70	(1,13)	2.13	30.2	361.4	0.75
(1,16)	2.54	38.3	457.2	0.64	**(1,16)**	2.00	30.2	361.4	0.78
(1,17)	2.32	35.5	425.7	0.51	(1,17)	2.15	35.6	426.8	0.48
(1,18)	2.39	30.5	364.6	0.49	(1,18)	2.48	30.0	358.8	0.57
(1,19)	2.31	30.3	362.4	0.51	(1,19)	2.45	30.1	360.8	0.52
(1,31)	1.44	30.1	359.6	0.76	(1,31)	2.04	45.2	357.9	0.65
(1,33)	3.06	27.0	323.1	0.65	(1,33)	2.91	26.1	311.3	0.60
(1,34)	2.65	35.7	427.3	0.57	(1,34)	2.02	35.7	427.1	0.54
(1,39)	2.79	43.4	520.0	0.61	(1,39)	2.10	43.5	521.8	0.58
(1,49)	1.97	26.2	313.3	0.61	(1,49)	1.87	26.1	312.2	0.60
(1,51)	2.91	31.0	365.5	0.51	(1,51)	1.62	30.7	367.1	0.42
(1,52)	2.98	41.2	494.8	0.76	(1,52)	1.76	40.0	478.0	0.81
(1,53)	2.14	35.5	425.6	0.32	(1,53)	2.30	35.2	422.4	0.37

[a] The units of the χ_0, χ_L, χ_m, and χ_q measures are the following: Å, Å, Å·u, and Å·e, respectively, where u is the unified atomic mass unit and e is the electron charge. nc stands for not converged.

(1,53) and (1,34) ones (of C_S, C_2, and C_1 symmetry, respectively) could be populated in ca. 15.6, 7.9, and 5.6, respectively (Table 1).

On the other hand, the main Chen et al. result for the $C_{58}B_2$ isomers cannot be confirmed at the B3LYP/6-31G** level. Indeed, they found that at the AM1 level, the most stable was the (1,2) $C_{58}B_2$ isomer of the C_v symmetry, and the other achiral isomer, the (1,4) one of the C_s symmetry, was almost equally populated: the energetic difference between the two isomers is ca. 0.5 kcal/mol.[32,33] However, calculations performed by using the DFT method show that the (1,4) is populated in 100% and population of the (1,2) is negligible (Table 1). Unexpectedly, repetition of the AM1 calculations with the Spartan 4 program[60] confirms the Chen et al. results, whereas the AM1 calculations with the Gaussian 09 program[56] confirm the DFT ones (Table 1). This would suggest that the AM1 codes either are somehow different, and parametrization of the method in the Gaussian 09 is corrected and the calculations yield results closer to these produced by the DFT codes, or the Spartan 4 optimization codes are more effective than these in Gaussian 09 and lead to lower heat of formation of the (1,2) $C_{58}B_2$ structure (Table 1). The judgment of the above statement is, however, not important for this paper as we assume the B3LYP/6-31G** results, used through this paper, as more reliable. Therefore, the partial conclusion based on the B3LYP/6-31G** calculations is that similarly to the $C_{58}N_2$ isomers, the achiral (1,4) $C_{58}B_2$ isomer is the most populated in the equilibrium mixture at 298 K. Yet, unlike the $C_{58}N_2$ isomer mixture, none of the $C_{58}B_2$ chiral structures is significantly populated.

3.2. Chirality of the $C_{58}B_2$ and $C_{58}N_2$ Structures. Fourteen of the $C_{58}X_2$ isomers belong to either the C_2 or C_1 point group of symmetry (Table 1) and are chiral.[61] The chirality can be measured: the measure should vanish for achiral structures and be greater than 0 for chiral ones. In 1992, Buda, Auf der Heyde, and Mislow[62] distinguished two categories of measures (i) aroused from a measure between a set of molecules and an achiral reference and (ii) aroused from a similarity measure

dx.doi.org/10.1021/jp208687c | J. Phys. Chem. A 2012, 116, 631–643

between a molecule (represented by a set of points) and its mirror image after arbitrary rotation. However, obviously, chirality measures based on chemical graph theory form a separate class of measures since they often do not refer to geometrical properties. Extensive reviews of chirality measures were done by Avnir, Zabrodsky Hel-Or, and Mezey in 1998,[63] Petitjean in 2003,[64] and Casanova and Casas in 2006[65] and of the graph theory chirality measures by Natarajan and Basak in 2009.[46]

Here, chirality is measured as minimized distance between two enantiomers represented as points in the Cartesian product of 3D Cartesian space R^3 and k-dimensional property space P^k, $R^3 \times P^k$ (for details, see eq 1 in the Calculations section). The calculations are performed by using our own CHIMEA program.[58] Roughly speaking, a chirality measure is a molecular asymmetry measure. If the properties of atoms in molecule are neglected, an n-atomic molecule is represented by a discrete set of n points in R^3 Cartesian space, and the χ_0 "pure" chirality measure expresses sheer geometrical asymmetry of the points. However, if some properties are attributed to the points, i.e., the property P^k space is not empty, even the achiral regular tetrahedron may become chiral if all its four points have distinct properties.

In this paper, we consider four geometry-related chirality measures: (i) χ_0—pure, (ii) χ_L—labeled, (iii) χ_m—mass, and (iv) χ_q—charge chirality measure. The labeled measure is connected to the fact that chemical elements differ from each other and are labeled by atomic symbols, and this changes the chirality of the geometrical points. Such a label can also have nonchemical meaning such as "color" used in the Petitjean approach.[66,67] Additionally, in the labeled measure we consider atom connectivity differences up to kth order (through k-bonds). The χ_m mass and the χ_q charge chirality measures result from different masses and charges of the atoms in molecules and are introduced by yet another weight assigned to Euclidean points (eq 1).

Generally, the χ_0, χ_L, χ_m, and χ_q measures are linearly independent because different weighting of the points leads to geometrically different superimposition of the two enantiomers and different chirality measure values. However, for the studied set of molecules, the χ_L and χ_m are strongly correlated, while the other pairs of measures, (χ_0; χ_L), (χ_0; χ_q), and (χ_L; χ_q), are linearly independent.

The main purpose for construction of a measure is to make use of it in some significant measurements. In the case of chiral molecules, it could be a selection of an important structure from the other isomers or an explanation for its specific activity. Here, the (1,16) $C_{58}N_2$ isomer is distinguished for the largest stability among chiral diazafullerenes. However, its χ_0 and χ_q chirality measures do not distinguish it from the other isomers: they are about average values of all the chiral $C_{58}N_2$ isomers. Yet, the $\chi_L(1,16)$ and $\chi_m(1,16)$ are the third largest (Table 2). On the other hand, the B3LYP/6-31G** calculations indicate that none of the chiral $C_{58}B_2$ isomers would be populated enough to be observed (Table 1).

Two series of fully analogous chiral compounds gave us an opportunity to perceive certain regular features of the studied measures (Figure 2). First, observe that there is no correlation between the pure χ_0 chirality measures of $C_{58}N_2$ and $C_{58}B_2$ isomers (Figure 2a). Second, the correlations of the labeled χ_L and mass χ_m chirality measures of two series of analogues are almost perfect (Figures 2b and 2c). Finally, the correlation between the charge χ_q chirality measures of the $C_{58}N_2$ and $C_{58}B_2$ isomers is weak but statistically significant (Figure 2d).

The lack of correlation for the pure χ_0 chirality measure means that this very parameter probably should not be used in predictions of the other molecular properties. This conclusion is quite surprising because the pure χ_0 chirality measure constitutes a natural base from which any other geometrical type of chirality measure can be systematically derived. Why does it happen? It is because in maximizing of an overlap of two enantiomeric sets of 60 indistinguishable points (by minimizing the distance between them (eq 1)) each point of one set can be referred to each point of the second set. Therefore, even a slight change of geometry, produced, for example, by incorporation of a different atom, can lead to settlement of a new minimum yielding quite a different value. Here, the effect is accelerated by the fact that the studied heterofullerenes are quite spherical and, in view of the pure chirality measure, are only very slightly chiral. Indeed, for an ordinary chiral molecule, for instance the 13-atom zwitterionic L-alanine molecule in crystal, the χ_0, χ_L, and χ_m measures are equal to ca. 4.0, 11.6, and 60.0,[68] respectively. Let us show the comparison in the light of the *specific (normalized) chirality measures*

$$\begin{aligned} \chi_0' &= \frac{1}{N}\chi_0 \\ \chi_L' &= \frac{1}{N}\chi_L \\ \chi_m' &= \frac{1}{M}\chi_m \\ \chi_q' &= \frac{1}{Q}\chi_q \end{aligned} \tag{5}$$

where N, M, and Q, are normalization factors equal to number of points, molar mass, and sum of absolute values of partial charges, respectively. Then, the $\chi'_0(1,16)$, $\chi'_L(1,16)$, and $\chi'_m(1,16)$ are equal to 0.022, 0.624, respectively, while for the zwitterionic L-alanine, the same measures are equal to 0.308, 0.892, and 0.673, respectively. Thus, the specific pure chirality measure of L-alanine molecule is ca. 14-times larger than that of the (1,16) isomer, whereas for the two molecules the χ'_L and χ'_m values are quite comparable.

On the other hand, there are excellent correlations between χ_L and χ_m measures taken for the $C_{58}N_2$ and $C_{58}B_2$ isomers (Figure 2b and c). In fact, they express the same relationship, as, for the $C_{58}X_2$ isomers, the χ_L and χ_m values are linearly dependent. Let us emphasize that for the $C_{58}X_2$ isomers, the χ_L and χ_m values demonstrate quite normal chiralities: the values are comparable with those of amino acids.[71] Where would such a difference between pure and labeled and mass chiralities could come from? To answer this question first recall that a geometrically achiral set, such as regular tetrahedron, may become chiral if all its four points would be pairwise distinguished by a property assigned to these points. This demonstrates a fundamental reason for linear independence of the pure and labeled and the pure and mass chirality measures. Now, for a given $C_{58}X_2$ molecule, for instance, the (1,16) $C_{58}N_2$ isomer, the strong constraint in calculating both χ_L and χ_m is the necessity to minimize either N1−N1′ and N16−N16′ or a pair of N1−N16′ and N16−N1′ distances, where "′" labels atoms in the enantiomer. Obviously, all the C(i)−C(j') distances have to be minimized (i and j' run over 1, 2, ..., 58 and 1′, 2′, ..., 58′ labels), but the constrains set on heteroatoms drastically cut off the degree of freedom of mutual maximal overlap (distance minimization) between enantiomers. This is why the overlap pattern is reproduced from one set of

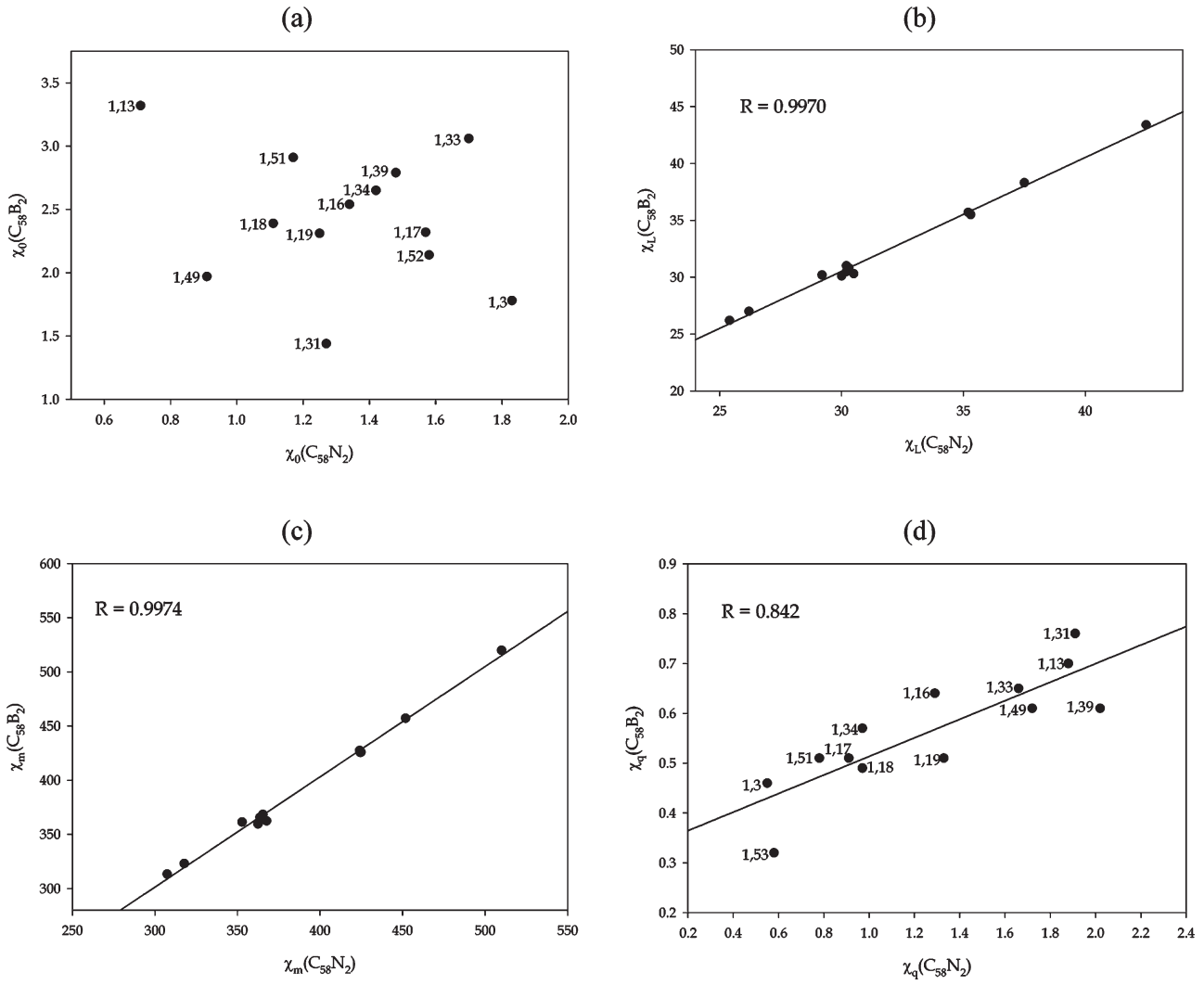

Figure 2. Relationships between geometrical chirality measures of the $C_{58}N_2$ isomers and their $C_{58}B_2$ analogues: pure measures (a), labeled measures (b), mass measures (c), charge measures (d).

isomers ($C_{58}N_2$) to their analogues ($C_{58}B_2$) and, as a consequence, there is the excellent correlations between $\chi_L(C_{58}N_2)$ and $\chi_L(C_{58}B_2)$ as well as $\chi_m(C_{58}N_2)$ and $\chi_m(C_{58}B_2)$ (Figure 2b and c).

Finally, let us explain why the correlation between $\chi_q(C_{58}N_2)$ and $\chi_q(C_{58}B_2)$ is much weaker than those for the labeled and mass chirality measures and stronger than that for the pure one (Figure 2d). Unlike for the pure chirality measure, in the charge chirality measure the points representing atoms have properties differentiating them. However, the differentiation is weaker than those of χ_L and χ_m. The χ_q are relatively small (Table 2, Figure 2d). Indeed, the partial charges assigned to atoms may change continuously usually between −1.0 and 1.0. This means that in some structures the charge of a heteroatom may be close to that of a C-atom, and this very pair may satisfy the minimization condition. However, it may happen that with the change of the heteroatom the heteroatom charge will be changed, and the previous condition is not satisfied anymore. Thus, in comparison with χ_L and χ_m, the enantiomer overlap pattern will be much more weakly reproduced between the sets of analogues and the correlation will be weaker. On the other side, the enantiomer overlap pattern will be sometimes reproduced, and the correlation will be much stronger than for the pure chirality measure.

A molecule changes its structure with the change of the electronic state. Therefore, having calculated triplet structures of the $C_{58}X_2$ isomers, it was intriguing for us whether chirality of the $C_{58}X_2$ heterofullerenes change significantly with the change of the electronic state from singlet to triplet or not. The chirality measures for the triplet $C_{58}X_2$ isomers calculated by using the UB3LYP/6-31G** method are gathered in Table 2, and the relationships between the measures determined for the $C_{58}N_2$ isomers in singlet and triplet states are presented in Figure 3. Unexpectedly, the χ_L and χ_m in the singlet and triple states are practically identical, the χ_q of the two states are very close to each other, and the χ_0 are practically uncorrelated (Figure 3). There is no controversy that the $C_{58}X_2$ isomers in singlet and triplet states are different: they exhibit different energies and energetic order (Table 1). Thus, why are the χ_L and χ_m values equal for the two states? This is because the $C_{58}X_2$ structures are so rigid that even change in electronic state changes the geometry but so slightly that this affects neither χ_L nor χ_m (Figure 3b and c). For weaker correlation of the χ_q measures of singlets and triplets (Figure 3d) as well as lack of correlation in the case of the χ_0 measures (Figure 3a) the same arguments hold true as those used above in comparison between measures of $C_{58}N_2$ and $C_{58}B_2$ series of

dx.doi.org/10.1021/jp208687c |J. Phys. Chem. A 2012, 116, 631–643

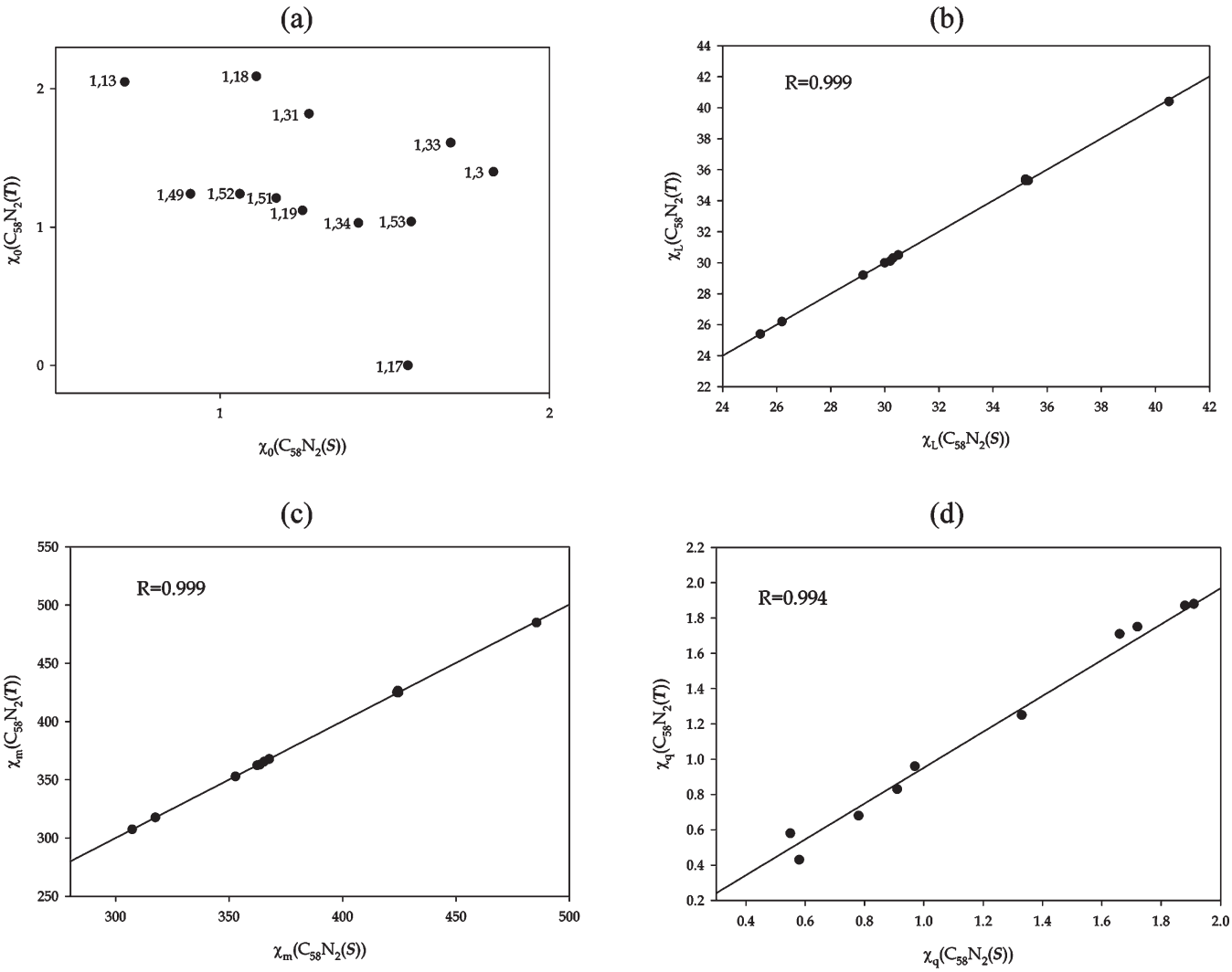

Figure 3. Relationships between geometrical chirality measures of the singlet state $C_{58}N_2$ isomers and their forms in the triplet state: pure measures (a), labeled measures (b), mass measures (c), and charge measures (d).

analogues. Additionally, the small values of the χ_q and χ_0 measures ($C_{58}X_2$ are almost spherical) may have caused some difficulties in finding the global minimum of the chirality measure, and a spread of points may be due to the existence of several local minima of these chirality measures.

3.3. The VCD Spectra. In 1998 Chen et al. predicted the electronic spectra of all the $C_{58}B_2$ and $C_{58}N_2$ structures using the INDO/CIS approach.[32,33] Here, we present the B3LYP/6-31G** prediction of the vibrational circular dichroism (VCD) spectra only for the chiral $C_{58}N_2$ and $C_{58}B_2$ isomers. The only chiral $C_{58}N_2$ isomer indicated to be populated in equilibrium conditions in identifiable amounts is the (1,16) isomer (Table 1), whereas no $C_{58}B_2$ isomer is predicted to be observed in these very conditions (Table 1). As the heterofullerenes can also be generated in far-from-equilibrium (nonequilibrium) conditions, we also show the strongest four positive and four negative VCD bands of the other chiral isomers (Table 3). Furthermore, the heterofullerenes can be successfully synthesized.[1−4,11,12] Nevertheless, if a strong motivation would have come from theoretical and computational studies, such as prediction of interesting magnetic, electric, elasticity, conductivity, second harmonic generation, and so forth, the synthetic chemists could certainly develop smart and effective asymmetric syntheses of selected heterofullerenes or efficient chiral separation techniques. Therefore, we provide the reader with the whole theoretical VCD spectra for the $C_{58}N_2$ and for the $C_{58}B_2$ isomers given in Tables 1SI−10S1 and 11SI−19SI, respectively.

The intensity of the VCD spectra is from approximately 100 to 1000 times weaker than that of the IR spectra.[69,70] Nevertheless, with the increasing development of the VCD spectrometers performance, this technique has become very fruitful in characterization of chiral compounds, successful in determination of absolute configuration, and promising in physicochemical studies.[71,72] This may be even more true for the VCD spectra of chiral heterofullerenes. Indeed, for all $C_{58}N_2$ molecules the (absolute value of) intensity of the strongest band exceeds 1000×10^{-44} esu^2 cm^2 and for some isomers exceeds $10\,000 \cdot 10^{-44}$ esu^2 cm^2, whereas that for the (1,49) isomer in the singlet state and (1,17) and (1,19) isomers in the triplet state is predicted to be greater than $40\,000 \cdot 10^{-44}$ esu^2 cm^2 (Table 3). For comparison, the strongest VCD bands of camphores, D-lactic acid monomer, and dihalogenoallenes do not exceed 70,[73,74] 100,[75] and 200[74] 10^{-44} esu^2 cm^2, respectively. On

dx.doi.org/10.1021/jp208687c |J. Phys. Chem. A 2012, 116, 631–643

Table 3. Harmonic Frequencies (cm^{-1}), IR Intensities (km/mol), Dipole Strength (10^{-40} esu^2 cm^2), and VCD Rotational Strengths (10^{-44} esu^2 cm^2) of the Strongest Four Positive and Four Negative VCD Bands of Each of the Chiral $C_{58}N_2$ and $C_{58}B_2$ Isomers in the Singlet and Triplet States Calculated at the (U)B3LYP/6-31G Level[a]**

	$C_{58}N_2$									$C_{58}B_2$							
	singlet state				triplet state					singlet state				triplet state			
isomer	freq	IR	dip	VCD	freq	IR	dip	VCD	isomer	freq	IR	dip	VCD	freq	IR	dip	VCD
(1,3)	1073	20.8	77.3	3106	1430	35.6	99.3	2456	(1,3)	1260	19.2	60.9	877	1504	6.3	16.8	136
	610	28.4	185.6	2007	625	5.2	33.1	750		1064	27.5	102.9	872	1179	9.0	30.3	120
	1335	20.4	60.9	1844	1589	9.2	23.0	720		1163	37.1	127.3	870	1164	2.9	9.9	105
	1205	17.2	56.9	1834	1243	4.3	13.9	544		1352	42.5	125.4	661	1081	4.6	16.8	99
	670	5.6	33.2	−628	647	13.0	80.3	−599		1455	12.1	33.2	−119	652	4.9	29.8	−76
	1195	30.2	100.7	−672	1185	2.8	9.4	−710		1319	9.3	28.1	−123	583	7.7	52.7	−93
	1424	30.9	86.4	−797	1371	8.2	23.8	−853		577	3.3	23.1	−124	1489	4.4	11.7	−99
	1427	45.7	127.8	−907	1225	13.6	44.4	−1376		1446	3.1	8.5	−141	1495	6.9	18.5	−114
(1,13)	635	25.0	156.8	1273	1450	32.9	90.4	2765	(1,13)	1514	28.7	75.6	323	1433	5.5	15.2	233
	1224	26.2	85.3	867	1370	1.9	5.6	1348		1472	8.5	22.9	195	971	3.8	15.4	113
	1362	6.8	19.9	855	1372	8.8	25.6	1332		1453	6.6	18.1	187	1418	4.2	11.9	109
	1205	13.7	45.3	832	1220	11.9	39.0	1028		1295	4.2	12.9	145	1440	14.6	40.3	104
	1445	33.1	91.3	−459	1173	13.8	47.0	−3964		1170	13.9	47.6	−287	1533	4.8	12.4	−126
	1428	56.4	157.7	−548	373	9.1	97.2	−5017		1075	13.5	49.9	−536	1538	4.4	11.5	−158
	1349	26.3	77.6	−1059	601	9.7	64.3	−6585		1437	19.0	52.6	−559	1395	3.8	10.7	−192
	664	18.8	112.9	−1126	1046	35.4	134.8	−12118		1465	20.0	54.5	−840	1169	16.5	56.4	−193
(1,16)	1450	39.3	108.1	624					(1,16)	567	5.0	35.5	290	1409	15.6	44.1	360
	1180	29.9	101.2	571						1425	2.2	6.2	179	1576	9.5	24.0	241
	1101	4.6	16.5	445						1380	2.4	7.1	165	1157	15.4	53.1	218
	1354	4.3	12.8	441						1179	17.5	59.3	155	1171	1.8	6.2	171
	1357	15.9	46.8	−945						1298	4.7	14.4	−273	1392	1.9	5.3	−401
	1201	38.5	127.8	−1590						751	19.3	102.5	−277	1082	4.8	17.7	−456
	1400	12.0	34.3	−1773						1449	50.1	138.1	−421	957	16.9	70.4	−536
	653	58.5	357.4	−1809						1255	13.9	44.1	−444	1273	11.9	37.1	−1322
(1,17)	1408	59.9	169.9	1619	932	108.9	466.1	45546	(1,17)	1384	10.3	29.7	372	1165	20.3	69.4	514
	1204	34.4	114.0	642	1167	16.2	55.3	7680		1442	3.2	8.8	333	1173	15.4	52.5	285
	1169	11.8	40.2	511	1294	24.2	74.7	5057		1439	18.2	50.5	315	1402	3.1	8.9	214
	1542	4.3	11.1	436	1233	9.9	32.0	4639		959	11.6	48.3	281	1418	3.6	10.0	191
	1345	24.4	72.4	−845	1204	5.3	17.4	−2860		1073	11.7	43.6	−506	1185	4.4	14.7	−148
	1419	55.6	156.3	−1243	1317	20.4	61.9	−3244		1175	15.8	53.5	−562	1275	2.0	6.4	−149
	1377	25.8	74.7	−1246	1225	29.8	97.1	−4073		1066	26.1	97.6	−957	1243	3.7	11.9	−180
	661	48.5	292.5	−1378	1373	16.4	47.7	−4190		1389	94.0	269.9	−1506	1420	6.2	17.4	−249
(1,18)	628	28.4	180.1	2261					(1,18)	1202	23.9	79.2	332	1314	7.4	22.4	360
	1367	13.0	37.9	2162						1564	13.4	34.2	296	1188	5.3	17.8	337
	1187	6.8	22.8	1705						1392	10.1	28.9	290	1244	4.2	13.5	322
	1406	42.3	119.9	1334						1159	3.9	13.3	194	1493	20.6	55.0	322
	667	8.7	51.9	−605						1197	16.7	55.5	−431	1193	0.8	2.7	−155
	1424	51.8	145.2	−731						1170	30.9	105.4	−436	1572	3.6	9.0	−176
	1401	42.3	120.4	−736						1188	20.3	68.2	−484	1096	3.8	13.8	−242
	1371	25.3	73.6	−1194						1078	21.3	79.0	−588	1307	12.3	37.5	−285
(1,19)	1087	16.6	61.0	4424	864	46.8	215.9	44070	(1,19)	1050	53.3	202.7	1999	1070	8.9	33.2	382
	1177	18.0	60.9	3368	1154	61.7	213.2	28052		1149	32.3	112.3	1306	1556	4.5	11.5	342
	1332	3.5	10.5	1397	1360	44.8	131.5	19580		1230	11.9	38.5	980	567	2.6	18.4	266
	1258	4.2	13.4	1193	1537	7.9	20.6	7927		200	5.4	107.1	446	1475	13.9	37.7	249
	1595	27.5	68.7	−676	1415	44.1	124.4	−8458		1097	9.3	33.8	−323	1159	11.8	40.7	−421
	1442	42.7	118.2	−844	1107	48.3	174.1	−14691		1576	7.1	17.9	−340	1258	12.8	40.6	−480
	1410	19.6	55.4	−1350	1487	34.3	92.0	−25242		1391	5.1	14.7	−361	1080	7.5	27.8	−595
	1397	48.9	139.7	−1574	1158	48.7	167.8	−37670		1415	3.3	9.3	−410	1387	15.8	45.5	−616
(1,31)	1379	49.9	144.3	4835	1064	33.0	123.6	7448	(1,31)	1265	35.4	111.6	1471	1480	15.9	43.0	318
	1213	22.0	72.2	1228	634	22.5	141.4	5780		1322	11.7	35.2	565	1483	22.4	60.2	304
	1510	8.3	21.8	859	1186	16.2	54.6	4020		1358	15.2	44.6	535	1185	9.5	32.0	175
	689	14.9	86.2	769	1397	22.6	64.5	3253		1220	8.0	26.1	485	1284	6.5	20.1	169
	318	56.7	710.4	−5126	690	5.0	29.0	−574		1515	44.7	117.8	−1418	1178	4.8	16.4	−146
	1309	43.7	133.2	−5252	1195	20.3	67.8	−650		1182	57.3	193.3	−1543	1576	3.9	9.8	−147
	1085	26.8	98.6	−5571	1408	9.5	27.0	−952		1068	11.7	43.7	−1850	1505	3.2	8.4	−199
	624	49.5	316.2	−7920	1422	30.8	86.5	−1082		1406	71.2	202.0	−2616	1406	2.7	7.6	−220

dx.doi.org/10.1021/jp208687c |J. Phys. Chem. A 2012, 116, 631–643

Table 3. Continued

	$C_{58}N_2$									$C_{58}B_2$								
	singlet state				triplet state					singlet state				triplet state				
isomer	freq	IR	dip	VCD	freq	IR	dip	VCD	isomer	freq	IR	dip	VCD	freq	IR	dip	VCD	
(1,33)	1420	50.9	143.0	2156	1425	74.1	207.3	4134	(1,33)	1265	13.1	41.3	622	1521	9.3	24.4	412	
	1224	15.6	51.0	2106	1401	9.2	26.3	2185		1438	6.4	17.7	438	1317	1.6	4.8	171	
	1587	9.8	24.7	937	658	5.1	30.6	1894		1284	12.5	38.8	430	1226	2.5	8.0	159	
	1435	35.3	98.3	720	1512	7.1	18.7	1110		1463	11.9	32.4	355	1319	7.0	21.2	149	
	1305	53.1	162.5	−13963	1567	7.2	18.3	−1963		1081	10.4	38.3	−1735	1557	9.6	24.6	−224	
	620	58.9	378.7	−15967	382	6.3	65.9	−3092		731	37.5	204.5	−2615	1385	4.2	12.2	−242	
	1196	82.1	273.9	−17904	1169	12.5	42.5	−3527		1427	58.7	164.1	−2942	1239	13.4	43.2	−280	
	1071	87.2	324.5	−23965	1071	10.2	38.2	−7539		1411	93.3	263.8	−3918	1215	5.7	18.8	−315	
(1,34)	1410	65.7	185.9	2286	1089	11.9	43.5	5899	(1,34)	1296	6.5	19.9	535	1390	7.1	20.5	257	
	1403	43.5	123.7	1946	1196	6.3	21.0	2236		1554	3.6	9.1	433	1412	5.0	14.2	212	
	1380	21.4	61.7	1497	629	6.8	43.0	2049		1507	5.7	15.0	376	1246	8.5	27.2	205	
	1360	12.1	35.4	820	377	5.7	59.9	1894		1436	9.9	27.4	346	1292	7.8	24.0	183	
	1236	12.5	40.3	−1655	1361	2.5	7.2	−500		1410	55.2	156.1	−1186	1578	7.1	17.8	−147	
	1418	45.2	127.2	−1681	1592	3.0	7.6	−518		1518	37.3	98.1	−1215	1250	9.0	28.8	−195	
	1335	11.8	35.4	−1999	1220	2.6	8.4	−643		1072	57.1	212.6	−2380	1183	3.1	10.3	−196	
	1331	19.0	57.1	−3495	1403	18.1	51.6	−1616		1399	95.8	273.2	−3773	1162	7.6	26.1	−199	
(1,39)	1209	162.2	535.0	11755					(1,39)	1068	116.1	433.7	14176	1208	21.7	71.5	270	
	1092	148.7	543.1	11295						1401	119.5	340.2	6857	577	3.5	24.1	234	
	1328	137.5	413.0	10204						670	39.1	232.6	6330	1287	1.5	4.6	132	
	639	137.9	860.8	10081						1407	94.1	266.9	6221	1079	1.2	4.4	115	
	1185	0.6	2.0	−869						1208	39.5	130.6	−338	1311	11.4	34.6	−157	
	699	20.9	118.9	−883						689	4.5	25.9	−511	1081	4.2	15.5	−224	
	1516	1.9	5.1	−961						1196	7.4	24.5	−1179	1225	6.8	22.1	−227	
	1392	40.6	116.3	−1708						1081	5.8	21.6	−1186	1244	4.8	15.4	−278	
(1,49)	1060	95.6	359.6	41123	593	5.0	33.8	1161	(1,49)	1379	42.2	122.0	2212	1534	21.7	56.5	576	
	1286	186.9	579.9	32719	1592	8.1	20.2	774		1358	21.6	63.3	1356	1087	8.5	31.1	431	
	615	57.9	375.5	25765	1185	6.3	21.1	631		1340	13.8	41.2	1136	1287	13.7	42.4	276	
	322	73.4	908.3	17598	1475	4.4	11.9	626		203	12.0	235.7	1020	1597	19.0	47.5	241	
	1381	51.1	147.8	−2735	1172	17.3	59.1	−6694		732	22.2	120.8	−1049	1199	15.1	50.2	−195	
	1305	27.3	83.3	−3109	1397	60.0	171.3	−7708		1274	31.7	99.2	−1117	770	10.9	56.4	−224	
	698	45.7	261.6	−3164	963	35.1	145.2	−9337		1399	95.3	271.5	−2350	1243	4.3	13.8	−235	
	1409	95.1	269.4	−7359	1029	76.1	295.0	−25707		1170	91.1	310.6	−2781	1517	11.8	31.1	−443	
(1,51)	1090	17.1	62.6	8381	1076	37.7	139.7	8001	(1,51)	1586	25.0	62.9	626	1163	14.6	50.2	641	
	1292	11.4	35.2	6801	652	26.4	161.7	6058		1466	5.8	15.8	311	1239	11.9	38.2	515	
	632	58.3	368.0	5293	1237	27.3	87.9	5878		1331	4.1	12.2	303	1400	12.6	35.9	407	
	332	8.5	101.4	3732	1223	85.5	279.0	4682		1609	3.2	8.0	297	1260	13.7	43.4	359	
	1380	6.0	17.2	−364	1587	6.4	16.0	−541		738	25.6	138.5	−1067	566	1.7	12.1	−155	
	703	11.9	67.5	−481	1580	21.0	52.9	−700		1294	26.9	83.0	−1634	1561	3.5	9.0	−167	
	1311	2.2	6.8	−561	1436	27.9	77.5	−1120		1423	22.8	63.8	−1643	1296	3.5	10.6	−175	
	1423	126.0	353.0	−1117	1424	17.4	48.9	−1313		1071	42.5	158.4	−2498	1076	4.6	16.9	−249	
(1,52)	623	62.3	399.1	15069	1419	74.5	209.5	933	(1,52)	1409	71.4	202.1	1922	1593	7.6	19.2	250	
	1076	49.7	184.3	14649	1453	10.5	28.8	413		1412	56.6	159.8	1471	1417	8.6	24.1	148	
	1310	62.3	189.8	13258	1236	12.2	39.3	336		1079	15.6	57.6	1200	1089	5.3	19.4	137	
	1255	31.8	100.9	7995	1444	23.8	65.8	277		1219	18.2	59.4	937	1297	2.3	7.1	125	
	1397	7.5	21.4	−1082	1275	10.8	33.9	−879		1313	7.3	22.1	−252	1596	6.1	15.2	−193	
	1187	14.3	48.0	−1122	1393	11.6	33.3	−920		1581	7.8	19.7	−320	1407	8.0	22.8	−204	
	698	20.8	118.8	−1341	665	11.0	66.0	−1115		1223	16.9	55.1	−418	1240	6.5	20.8	−252	
	1418	54.0	152.1	−1971	1412	49.6	140.0	−3182		1527	24.3	63.4	−620	1421	8.8	24.6	−268	
(1,53)	1328	79.8	239.8	8476	1420	21.3	59.8	1216	(1,53)	1416	133.1	375.0	2194	1735	46.8	107.5	14454	
	651	81.4	498.5	7632	1442	17.3	48.0	708		1513	20.4	53.9	775	1568	32.4	82.4	2288	
	1390	36.7	105.3	3469	1585	26.6	66.8	501		1484	10.4	28.0	692	1492	8.5	22.6	1960	
	1338	21.4	63.8	2603	1519	7.6	20.0	413		1084	8.3	30.6	655	1109	14.3	51.6	1660	
	1428	30.8	86.0	−1395	1100	3.3	12.1	−1616		1180	15.4	52.0	−471	380	11.2	117.6	−4126	
	698	27.5	157.3	−1443	1391	17.2	49.5	−2369		1424	14.0	39.2	−520	148	11.3	304.5	−6493	
	1189	31.2	104.7	−1776	652	14.9	91.1	−2492		1302	18.3	56.1	−534	1298	19.6	60.1	−10027	
	1399	17.6	50.1	−1927	1410	141.3	399.7	−3144		1213	26.1	85.9	−962	1045	63.8	243.6	−16215	

[a] Full theoretical spectra can be found in the Supporting Information file.

dx.doi.org/10.1021/jp208687c |J. Phys. Chem. A 2012, 116, 631–643

the other hand the VCD spectra of the chiral $C_{58}B_2$ isomers are much less intense than those of their N-analogues (Table 3, Tables 6SI−10SI). For example, the strongest band of the (1,16) isomer in the singlet state is equal to only -444×10^{-44} esu^2 cm^2, whereas the strongest one of the (1,13) triplet equals only 233×10^{-44} esu^2 cm^2. Nevertheless, most of the isomers have at least one quite strong VCD band (Table 3).

In conclusion of this section, we have shown that if a enantiopure $C_{58}N_2$ or a $C_{58}B_2$ isomer would be separated it could be successfully detected and, possibly, determined thanks to strong VCD bands with pattern specific to each enantiomer (Tables 3 and 1SI−19SI). In particular, the most populated chiral (1,16) $C_{58}N_2$ isomer can be detected based on three negative VCD bands at 1400, 1200, and 650 cm^{-1} of intensities exceeding 1500×10^{-44} esu^2 cm^2 (Table 3). Also, if somehow the most populated (1,52) $C_{58}N_2$ triplet would be isolated, it could be identified based on two negative VCD bands at ca. 1410 and 665 cm^{-1} of intensities exceeding 3000 and 1000×10^{-44} esu^2 cm^2, respectively.

4. CONCLUSIONS

The systematic investigation of all the 23 IPR conserving isomers of the $C_{58}N_2$ and $C_{58}B_2$ heterofullerenes in the singlet and triplet states was performed at the B3LYP/6-31G** level. It appeared that the two most populated singlet states of $C_{58}N_2$ isomers are the same as found earlier by Chen et al. (*J. Chem. Soc., Faraday Trans.* **1998**, *94*, 2269−2276) at the AM1 level, whereas out of two $C_{58}B_2$ isomers that are the most stable in the Chen et al. study only one was confirmed to be very stable at the DFT level. According to our DFT calculations of the Gibbs free energies, the achiral (1,4) $C_{58}N_2$ isomer of C_s symmetry is populated in ca. 95.8% and the chiral (1,16) one of the C_2 symmetry is populated in ca. 3.3%, while the achiral 1,4 $C_{58}B_2$ is populated in 100%. All the $C_{58}N_2$ and $C_{58}B_2$ triplet state isomers are less stable than the two and one most stable singlets, respectively. Thus, out of 14 possible chiral $C_{58}N_2$ isomers only the (1,16) one seems to be obtainable in reasonable amounts, whereas for the $C_{58}B_2$ chiral structures none seems to be significantly populated in equilibrium mixture at normal conditions.

For the two series of analogous chiral molecules several geometry-derived chirality measures were investigated. It was found that there is no correlation between pure geometrical chirality measures of the $C_{58}N_2$ and $C_{58}B_2$ analogues, the labeled and mass-weighted chirality measures correlate with $R = 0.99$, and correlation based on partial-charge-weighted measure is weaker but statistically significant. The same holds true for correlations between chirality measures of the $C_{58}X_2$ molecules in singlet and triplet states. Lack of correlation of pure chirality measures is due to the fact that in calculating the distance between enantiomers each point of a heterofullerene (representing an atom) can be referred to each point of the enantiomer: the points are indistinguishable. Therefore, even a slight change of geometry, produced, for example, by incorporation of different atom, can lead to settlement of a new minimum yielding quite a different value. Better correlations in the case of the labeled, mass, and charge chirality measures are due to constrains in the minimization coming from necessity of measuring distances between selected points possessing a distinguished property—the heteroatoms. In conclusion we suggested that pure geometrical chirality measure should not be used in QSAR predictions of the other molecular properties, while the labeled and mass-weighted measures are promising QSAR descriptors of the molecular chirality.

For all the chiral structures we have predicted their vibrational circular dichroism spectra and have given the most characteristic VCD bands. It was shown that if an enantiopure $C_{58}N_2$ or a $C_{58}B_2$ isomer would be separated it could be successfully detected and, possibly, determined thanks to strong VCD bands with a pattern specific to each enantiomer. In particular, the most populated chiral (1,16) $C_{58}N_2$ isomer can be detected based on three negative VCD bands at 1400, 1200, and 650 cm^{-1} of intensities exceeding 1500×10^{-44} esu^2 cm^2.

■ ASSOCIATED CONTENT

Supporting Information. B3LYP/6-31G**-calculated harmonic frequencies, IR intensities, dipole strengths, and VCD rotational strengths for all studied structures (Tables 1S−19S). This material is available free of charge via the Internet at http://pubs.acs.org.

■ AUTHOR INFORMATION

Corresponding Author

*Tel. (+48)22-568-24-21; fax (+48)22-568-22-93; e-mail janek@il.waw.pl.

■ ACKNOWLEDGMENT

This work was partially supported by the Grant of Ministry of Science and Higher Education in Poland for statutory activity of the Industrial Chemistry Research Institute in 2011. The computational grants G19-2 and G19-4 from the Interdisciplinary Center of Mathematical and Computer Modeling (ICM) at the Warsaw University are gratefully acknowledged.

■ REFERENCES

(1) Hummelen, J. C.; Bellavia-Lund, C.; Wudl, F. *Top. Curr. Chem.* **1999**, *199*, 93–134.
(2) Hirsch, A.; Brettreich, M. *Chemistry and Reactions*, 2nd ed.; Wiley-VCH: Weinheim, Germany, 2005; Chapter 12.
(3) Hirsch, A.; Nuber, B. *Acc. Chem. Res.* **1999**, *32*, 795–804.
(4) Vostrowsky, O.; Hirsch, A. *Chem. Rev.* **2006**, *106*, 5191–5207.
(5) Guo, T.; Jin, C.; Smalley, R. E. *J. Phys. Chem.* **1991**, *95*, 4948–4950.
(6) Smalley, R. E. Hammond, G. S.; Kuck V. J., Eds. *ACS Symp. Ser.* **1992**, *481*, 141-159.
(7) Chai, Y.; Guo, T.; Jin, C. M.; Haufler, R. E.; Chibante, L. P. F.; Fure, J.; Wang, L. H.; Alford, J. M.; Smalley, R. E. *J. Phys. Chem.* **1991**, *95*, 7564–7568.
(8) Hummelen, J. C.; Knight, B.; Pavlovich, J.; González, R.; Wudl, F. *Science* **1995**, *269*, 1554–1556.
(9) Nuber, B.; Hirsch, A. *Chem. Commun* **1996**, 1421–1422.
(10) Yu, R.; Zhan, M.; Cheng, D.; Yang, S.; Liu, Z.; Zheng, L. *J. Phys. Chem.* **1995**, *99*, 1818–1819.
(11) Reuther, U.; Hirsch, A. *Carbon* **2000**, *38*, 1539–1549.
(12) von Delius, M.; Hauke, F.; Hirsch, A. *Eur. J. Org. Chem.* **2008**, *2008*, 4109–4119.
(13) Kimura, T.; Sugai, T.; Shinohara, H. *Chem. Phys. Lett.* **1996**, *256*, 269–273.
(14) Esfarjani, K.; Ohno, K.; Kawazoe, Y *Phys. Rev. B* **1994**, *50*, 17830–17836.
(15) Esfarjani, K.; Ohno, K.; Kawazoe, Y *Solid State Commun.* **1996**, *97*, 539–542.
(16) Nakamura, T.; Ishikawa, K.; Yamamoto, K.; Ohana, T.; Fujiwara, S.; Koga, Y. *Phys. Chem. Chem. Phys.* **1999**, *1*, 2631–2633.

(17) Fye, J. L.; Jarrold, M. F. *J. Phys. Chem. A* **1997**, *101*, 1836–1840.
(18) Pellarin, M.; Ray, C.; Mélinon, P.; Lermé, J.; Vialle, J. L.; Kéghélian, P.; Perez, A.; Broyer, M. *Chem. Phys. Lett.* **1997**, *277*, 96–104.
(19) Ohtsuki, T.; Ohno, K.; Shiga, K.; Kawazoe, Y.; Maruyama, Y.; Masumoto, K. *Phys. Rev. B* **1999**, *60*, 1531–1534.
(20) Sjöström, H.; Stafström, S.; Boman, M.; Sundgren, J.-E. *Phys. Rev. Lett.* **1995**, *75*, 1336–1339.
(21) Hultman, L.; Stafström, S.; Czigany, Z.; Neidhardt, J.; Hellgren, N.; Brunell, I. F.; Suenaga, K.; Colliex, C. *Phys. Rev. Lett.* **2001**, *87*, 225503−1–225503−4.
(22) Xie, R.-H.; Bryant, G. W.; Sun, G.; Kar, T.; Chen, Z.; Smith, V. H., Jr.; Araki, Y.; Tagmatarchis, N.; Shinohara, H.; Ito, O. *Phys. Rev. B* **2004**, *69*, 201403–1 - 201403−4.
(23) Kaneko, T.; Li, Y.; Nishigaki, S.; Hatakeyama, R. *J. Am. Chem. Soc.* **2008**, *130*, 2714–2715.
(24) Jing-Nan, L.; Bing-Lin, G.; Ru-Shan, H. *Solid State Commun.* **1992**, *84*, 807–810.
(25) Rosén, A.; Wästberg, B. *Surf. Sci.* **1992**, *269*−*270*, 1121–1128.
(26) Kurita, N.; Kobayashi, K.; Kumahora, H.; Tago, K. *Phys. Rev. B* **1993**, *48*, 4850–4854.
(27) Liu, M.; Wang, Z. D.; Dong, J.; Xing, D. Y. *Z. Phys. B* **1995**, *97*, 433–437.
(28) Wang, S.-H.; Chen, F.; Fann, Y.-C.; Kashani, M.; Malaty, M.; Jansen, S. A. *J. Phys. Chem.* **1995**, *99*, 6801–6807.
(29) Kashtanov, S.; Rubio-Pons, O.; Luo, Y.; Ågren, H.; Stafström, S.; Csillag, S. *Chem. Phys. Let.* **2003**, *371*, 98–104.
(30) Jensen, L.; Duijnen, P. Th.; Snijders, J. G.; Chong, D. P. *Chem. Phys. Lett.* **2002**, *359*, 524–529.
(31) Ewels, C. P. *Nano Lett.* **2006**, *6*, 890–895.
(32) Chen, Z.; Ma, K.; Pan, Y.; Zhao, X.; Tang, A.; Feng, J. *J. Chem. Soc., Faraday Trans.* **1998**, *94*, 2269–2276.
(33) Chen, Z.; Ma, K.; Chen, L.; Zhao, H.; Pan, Y.; Zhao, X.; Tang, A.; Feng, J. *J. Mol. Struct. (Theochem)* **1998**, *452*, 219–225.
(34) Fan, X.; Zhu, Z.; Liu, L.; Shen, Z.; Kuo, J.-L. *Commun. Comput. Phys.* **2010**, *8*, 289–303.
(35) Ren, A.; Feng, J.; Sun, X.; Li, W.; Tian, W.; Sun, C.; Zheng, X.; Zerner, M. C. *Int. J. Quantum Chem.* **2000**, *78*, 422–436.
(36) Caglioti, L.; Micskei, K.; Pályi, G. *Chirality* **2011**, *23*, 65–68.
(37) *Chirality in Drug Research*; Francotte, E., Lindner, W., Eds.; Wiley-VCH: Weinheim, Germany, 2006.
(38) Christmann, M.; Bräse, S. *Asymmetric Synthesis—The Essentials*, 2nd ed.; Wiley-VCH: Weinheim, Germany, 2007.
(39) http://nobelprize.org/nobel_prizes/chemistry/laureates/2001/public.html.
(40) Lemaire, M. *Pure Appl. Chem.* **2004**, *76*, 679–688.
(41) Ettl, R.; Chao, I.; Diederich, F.; Whetten, R. L. *Nature (London)* **1991**, *353*, 149–153.
(42) Diederich, F.; Whetten, R. L.; Thilgen, C.; Ettl, R.; Chao, I.; Alvarez, M. M. *Science* **1991**, *254*, 1768–1770.
(43) Thilgen, C.; Diederich, F. *Chem. Rev.* **2006**, *106*, 5049–5135.
(44) Ashrafi, A. R.; Ghorbani, M. *J. Serb. Chem. Soc.* **2010**, *71*, 361–368.
(45) Katritzky, A. R.; Kuanar, M.; Slavov, S.; Hall, C. D.; Karelson, M.; Kahn, I.; Dobchev, D. A. *Chem. Rev.* **2010**, *110*, 5714–5789.
(46) Natarajan, R.; Basak, S. C. *Curr. Comput.-Aided Drug Des.* **2009**, *5*, 13–22.
(47) Yang, C.; Zhong, C. *QSAR Combust. Sci.* **2005**, *24*, 1047–1055.
(48) Natarajan, R.; Basak, S. C; Balaban, A. T; Klun, J. A; Schmidt, W. F *Pest. Manag. Sci.* **2005**, *61*, 1193–1201.
(49) Zayit, A.; Pinsky, M.; Elgavi, H.; Dryzun, C.; Avnir, D. *Chirality* **2011**, *23*, 17–23.
(50) Saito, R.; Dresselhaus, G.; Dresselhaus, M. S. *Physical Properties of Carbon Nanotubes*; Imperial College Press: London, U.K.; 1998.
(51) Kaneko, T.; Li, Y.; Nishigaki, S.; Hatakeyama, R. *J. Am. Chem. Soc.* **2008**, *130*, 2714–2715.
(52) Becke, A. D. *J. Chem. Phys.* **1993**, *98*, 5648–5652.
(53) Burke, K.; Perdew, J. P.; Wang, Y. In *Electronic Density Functional Theory: Recent Progress and New Directions*; Dobson, J. F., Vignale, G., Das, M. P., Eds.; Plenum: New York, 1998.
(54) Petersson, G. A.; Al-Laham, M. A. *J. Chem. Phys.* **1991**, *94*, 6081–90.
(55) Frisch, M. J.; Trucks, G. W.; Schlegel, H. B.; Scuseria, G. E.; Robb, M. A.; Cheeseman, J. R.; Scalmani, G.; Barone, V.; Mennucci, B.; Petersson, G. A. et al. *Gaussian 09*, revision B.01; Gaussian, Inc.: Wallingford, CT, 2009.
(56) Cheeseman, J. R.; Frisch, M. J.; Devlin, F. J.; Stephens, P. J. *Chem. Phys. Lett.* **1996**, *252*, 211–220.
(57) Jamróz, M. H. *VEDA 4 program for Vibrational Energy Distribution Analysis*; Warsaw, Poland, 2004−2010; www.smmg.pl.
(58) Jamróz, M. H. *CHIMEA—Program Calculating Discret Chirality Measures of Molecules*; Warsaw, Poland, 2010.
(59) Godly, E. W.; Taylor, R. *Pure Appl. Chem.* **1997**, *69*, 1411–1434.
(60) SPARTAN 5.1.3, Wavefunction Inc., 18401 Von Karman Avenue, Suite 370, Irvine, CA 92612; http://www.wavefun.com/.
(61) *Basic terminology of stereochemistry*; IUPAC Recommendations 1996, PAC, **1996**, Vol. *68*, pp 2193, 2203; Blue Book, p 479.
(62) Buda, A. B.; Auf der Heyde, T.; Mislow, K. *Angew. Chem., Int. Ed. Engl.* **1992**, *31*, 989–1007.
(63) Avnir, D.; Hel-Or, H.; Mezey, P. Symmetry and Chirality: Continuous Measures. In *The Encyclopedia of Computational Chemistry*; Schleyer, P. V., Allinger, N. L., Clark, T., Gasteiger, J., Kollman, P. A., Schaefer, H. F., III, Schreiner, P. R., Eds.; Wiley: Chichester, U.K., 1998; Vol 4, pp 2890−2901; http://cs.haifa.ac.il/hagit/papers/CCencyclopedia9.
(64) Petitjean, M. *Entropy* **2003**, *5*, 271–312.
(65) Casanova i Casas, D. *Mesures de forma i simetria en química: algorismes i aplicacions*. Ph.D. Thesis under the supervision of S. Á. Reverter, P. A. Cahner, Universitat de Barcelona, Spain, 2006.
(66) Petitjean, M. *J. Math. Phys.* **2002**, *43*, 4147–4157.
(67) Petitjean, M. *Symmetry: Cult. Sci.* **2006**, *17*, 197–205.
(68) Jamróz, M. H.; Rode, J. E.; Ostrowski, S.; Dobrowolski, J. Cz. *On Chirality of Amino Acids*, presentation at the CD2011 conference, Oxford, July, 24−28th, 2011, and the article in preparation.
(69) Buckingham, A. D. *Faraday Discuss.* **1994**, *99*, 1.
(70) Autschbach, J. *Chirality* **2009**, *21*, E116–E152.
(71) Nafie, L. A.; Dukor, R. K.; Freedman, T. B. Vibrational Circular Dichroism. In *Handbook of Vibrational Spectroscopy*; Chalmers, J. M., Griffiths, P. R., Eds.; John Wiley & Sons Ltd.: Chichester, U.K., 2002; pp 731−744.
(72) Sadlej, J.; Dobrowolski, J. Cz.; Rode, J. E. *Chem. Soc. Rev.* **2010**, *39*, 1478–1488.
(73) Kingman, J. F. C.; Taylor, S. J. *Introduction to measure and probability*; Cambridge University Press: Cambridge, U.K., 1966.
(74) Longhi, G.; Abbate, S.; Gangemi, R.; Giorgio, E.; Rosini, C. *J. Phys. Chem. A* **2006**, *110*, 4958–4968.
(75) Abbate, S.; Burgi, L. F.; Gangemi, F.; Gangemi, R.; Lebon, F.; Longhi, G.; Pultz, V. M.; Lightner, D. A. *J. Phys. Chem. A* **2009**, *113*, 11390–11405.
(76) Sadlej, J.; Dobrowolski, J. Cz.; Rode, J. E.; Jamróz, M. H. *Phys. Chem. Chem. Phys.* **2006**, *8*, 101–113.
(77) Rode, J. E.; Dobrowolski, J. Cz. *J. Mol. Struct. (Theochem)* **2003**, *635*, 151–159.